Study of Redox Processes in Zeolite Y-Associated 2,4,6-Triphenylthiopyrylium Ion by Square Wave Voltammetry

Antonio Doménech,*,† Hermenegildo García,‡ Mercedes Alvaro,‡ and Esther Carbonell‡

Department of Analytical Chemistry, University of Valencia, Dr. Moliner 50, 46100 Burjasot,Valencia, Spain, and Institute of Chemical Technology CSIC-UPV, Polytechnical University of Valencia, Cno. Vera s/n. Ap. 22012, 46071 Valencia, Spain

Received: November 1, 2002

The electrochemical responses of 2,4,6-triphenylthiopyrylium ion (TTP^+) in solution and attached to zeolite Y (TTP@Y) are described using cyclic and square wave voltammetries upon immersion of zeolite-modified polymer film electrodes in MeCN ($LiClO_4$, Et_4NClO_4, and BuN_4PF_6 electrolytes) and aqueous ($LiNO_3$, $NaNO_3$, and KNO_3 electrolytes) media. The electrochemistry of TTP@Y in contact with Bu_4NPF_6/MeCN is identical to that of TTP(BF_4) in solution, with reduction processes at −0.25, −0.74, and −1.36 V vs SCE, and oxidation steps at +0.85 and +1.11 V. This response differs from those obtained for TTP@Y in Et_4NClO_4/MeCN and $LiClO_4$/MeCN electrolytes. In contact with aqueous electrolytes, TTP@Y displays a reversible one-electron transfer at −0.25 V in contrast with the adsorptive behavior observed for solid TTP(BF_4) attached to graphite, platinum, and gold electrodes. For TTP@Y, two different thick-layer and thin-layer responses are obtained which can be attributed to different topological redox isomers associated to different sites in the zeolite boundary. Thermochemical data for such processes are obtained from the temperature dependence of electrode potentials.

1. Introduction

The ability of zeolite molecular sieves to incorporate electrochemically active ions proved to be useful in the development of electrocatalytic systems[1] and in the design of analytical sensors.[2]

To describe the mechanism of charge transfer at zeolite-modified electrodes extrazeolitic, intrazeolitic, and surface-mediated electron-transfer processes have been described.[3,4] Following Shaw et al.,[5] in the extrazeolitic mechanism, the electron transfer process takes place outside of the zeolite following ion exchange of electroactive species with electrolyte cations. The intrazeolitic mechanism involves electron transfer processes affecting electroactive species located in the supercages of the outer cavities or subsurface zones of the zeolite. In the surface-mediated electron transfer mechanism, electroactive species of the zeolite surface undergo initial electron transfer and subsequently experience outer-sphere electron-transfer processes with intrazeolite species.[6−8]

The exact nature of the electrochemical processes involving zeolite-associated species has been the subject of discussion.[9−12] Thus, Baker et al. have claimed the character exclusively extrazeolitic of electrode processes on the basis of their studies on silver zeolite-modified electrode,[13−16] and zeolite-associated methyl viologen.[17] Bedioui et al. have advocated for the operativity of an intrazeolitic mechanism for describing the electrochemistry of different zeolite-encapsulated transition metal complexes,[18−21] whereas Calzaferri et al. have discussed the compatibility of such a mechanism with experimental data for methyl viologen-zeolite electrodes,[22] silver, and copper zeolite-modified electrodes,[22−25] with account of possible intrazeolite electron transport and intrazeolite ion transport mechanisms.[25]

More recently, Bessel and Rolison have studied the electrochemistry of zeolite-modified electrodes and heterogeneous dispersions of zeolite-encapsulated transition metal complexes providing evidence for electroactivity restricted to boundary-associated species.[26,27] These authors develop the idea that different electrochemical redox isomers may be responsible for the observed electrochemistry, using a terminology analogous to that proposed by Turro and García-Garibay[28] in the study of zeolite-associated photochemical probes. Electrochemical data consistent with the presence of different topological redox isomers in the case of Y zeolite-asociated Mn(salen)N_3 complex (salen = *trans*-(*R*,*R*)-1,2-bis(salicyldeneamino)cyclohexane) have been presented.[29]

In this context, we have studied the voltammetric response of reactive bulky organic cations which are stabilized upon confinement into zeolites, attempting to acquire more information on the electrochemistry of zeolite-associated species. It is known that relatively bulky molecules can be accommodated into the internal voids of zeolites through "ship-in-a-bottle" synthesis provided that their size is smaller than the void dimensions. The inert host framework protects reactive guest molecules from the attack of external reagents, enhancing enormously their persistence.[30,31] This effect has been previously described for 2,4,6-triphenylpyrylium ion (TP^+) encapsulated into zeolite Y,[32,33] and anthracene and thianthrene radical ions incorporated within pentasil and mordenite zeolites.[34,35] Electrodes modified with zeolite-associated 2,4,6-triphenylpyrylium ions can be used as selective electrochemical sensors for the determination of catecholamine neurotransmitters.[36,37]

In the current report, the electrochemistry of 2,4,6-triphenylthiopyrylium ion (TTP^+) associated to zeolite Y is studied using zeolite-modified polymer film electrodes immersed in

* Corresponding author. E-mail: antonio.domenech@UV.es.
† University of Valencia.
‡ Polytechnical University of Valencia.

10.1021/jp0223657 CCC: $25.00
Published on Web 03/07/2003

different MeCN and aqueous media. The electrochemical response of zeolite Y-associated thiopyrylium ions (TTP@Y) is compared with that of solutions of $TTP(BF_4)$ and TTP^+ adsorbed on glassy carbon, platinum, and gold electrodes as well as that of solid $TTP(BF_4)$ attached to solid electrodes. Square wave voltammetry (SQWV) has been used because of its inherently high analytical sensitivity and its immunity to capacitive effects. Since this technique enables the simultaneous inspection of the reduction and the oxidation processes it provides considerable insight into the mechanism of electrode reaction.[38]

2. Experimental Section

2.1. Materials and Chemicals. $TTP(BF_4)$ was prepared following the procedure previously reported.[39] The synthesis and nonelectrochemical characterization of 2,4,6-triphenylpyrylium ion in the intracrystalline cages of zeolite Y was carried out, as already reported,[39] following the scheme previously developed for zeolite encapsulation of 2,4,6-triphenylpyrylium ion.[32,33]

Commercially available Paraloid B72, an ethyl acrylate (70%)−methyl acrylate (30%) copolymer (P[EMA/MA]) was selected for polymer-film electrode preparation because of its mechanical stability and ability to form porous films able to adhere the zeolite microparticles to the electrode surface.[29,37] This facilitates the direct contact between the zeolite particles and the substrate electrode, which is a crucial aspect for studying the electrochemistry of zeolite-associated species.[9−12,17,22]

2.2. Modified Electrode Preparation. Zeolite-modified electrodes were prepared, as previously described,[29,37] by transferring a few microliters (typically 50 μL) of a dispersion of the zeolite (10 mg) in acetone (5 mL) to the surface of a freshly polished glassy carbon electrode and allowing the coating to dry in air. After the electrode surface was air-dried, one drop of a solution of the acrylic resin (1%) in acetone was added and the modified electrode was air-dried. The coatings examined contained 0.2−5.5 mg/cm^2 of the dry zeolite.

$TTP(BF_4)$-attached electrodes were prepared following the general methodology described by Scholz et al. in the context of solid-state electrochemistry.[40] The sample (1−2 mg) was powdered in an agate mortar and pestle, and placed on a glazed porcelain tile forming a spot of finely distributed material. Then the lower end of the electrode was gently rubbed over that spot of sample and finally cleaned with a tissue paper to remove ill-adhered particles. Additional experiments were performed on TTP^+-adsorbed electrodes. Following the methodology described by Lever et al.,[41] a freshly polished glassy carbon or platinum electrode was soaked in a dilute solution of $TTP(BF_4)$ (0.20 mM) in MeCN for 30 s and then washed and transferred to pure supporting electrolyte to record the voltammograms.

2.3. Instrumentation and Procedures. Cyclic voltammograms (CVs) and square wave voltammograms (SQWVs) were performed with a BAS CV50W equipment. Additional linear potential scan voltammograms (LSVs) were performed with a Metrohm E506 polarecord. A standard three-electrode arrangement was used with a platinum auxiliary electrode and a saturated calomel reference electrode (SCE) in a thermostated cell. For experiments in MeCN the reference electrode was separated from the solution using a capillary salt bridge. As basal electrodes, glassy carbon (BAS MF 2012, geometrical area 0.071 cm^2), platinum (BAS MF 2013, geometrical area 0.017 cm^2), and gold (BAS MF 2014, geometrical area 0.017 cm^2) electrodes were used. Experiments were conducted in aqueous media using $LiNO_3$, $NaNO_3$, and KNO_3 (all Panreac reagents) as supporting electrolytes in concentrations from 0.01 to 1.0 M. Experiments in MeCN were performed with $LiClO_4$, Et_4NClO_4, and Bu_4NPF_6 (all supported by Aldrich) electrolytes in the 0.01−0.25 M concentration range. All electrochemical measurements were performed in well-deaerated solutions under an atmosphere of argon.

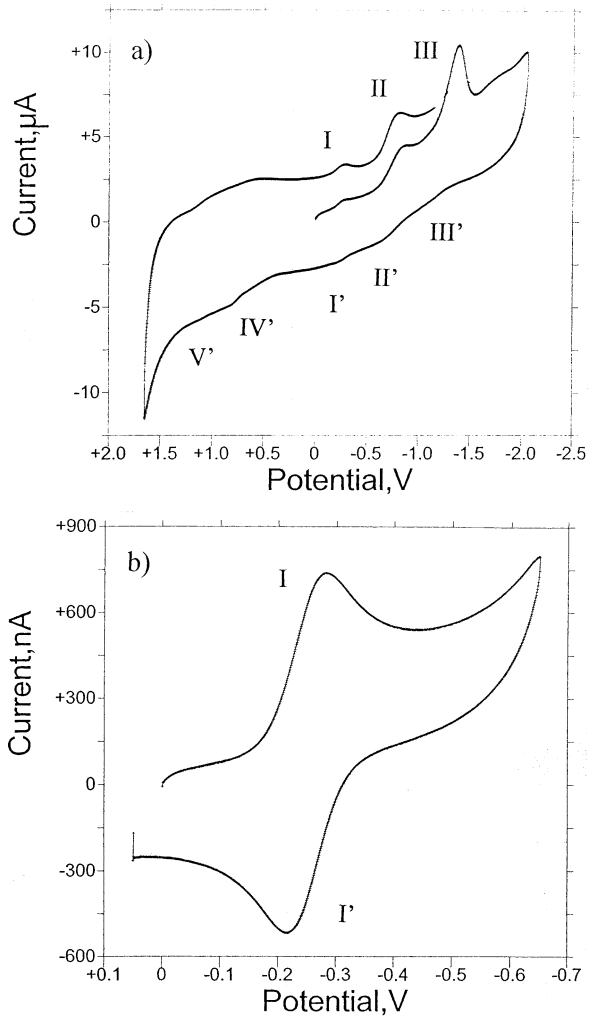

Figure 1. CVs at the GCE of a solution of $TTP(BF_4)$ (0.1 mM) in MeCN (0.10 M Et_4NClO_4). (a) Potential range: +1.65/−2.05 V; (b) potential range +0.05/−0.65 V. Potential scan rate 100 mV/s.

3. Results

3.1. Electrochemistry of TTP^+ in MeCN Solution. As shown in Figure 1a, the CV of $TTP(BF_4)$ dissolved in MeCN (0.10 M Et_4NClO_4) in the potential region from +1.65 to −2.05 V presents a relatively complicated profile, with cathodic peaks at −270 (I), −855 (II), and −1380 mV (III), whose anodic counterparts (respectively, I′, II′, III′) are ill-defined. On scanning the potential in the positive direction, anodic peaks at +840 (IV′) and +1100 mV (V′) appear. In the potential range from +0.05 to −0.65 V, peaks I/I′ conform to an apparently reversible one-electron couple with peak potentials of −270 mV and −210 mV, corresponding to a formal electrode potential of −240 mV (see Figure 1b). The peak current is proportional to the square root of the potential scan rate, indicating that the electronde process is diffusion-controlled. This response remains unchanged upon repetitive cycling the potential scan, suggesting that no coupled chemical reactions appear. In agreement with CV data, SQWVs exhibit only one peak at −250 mV, the peak

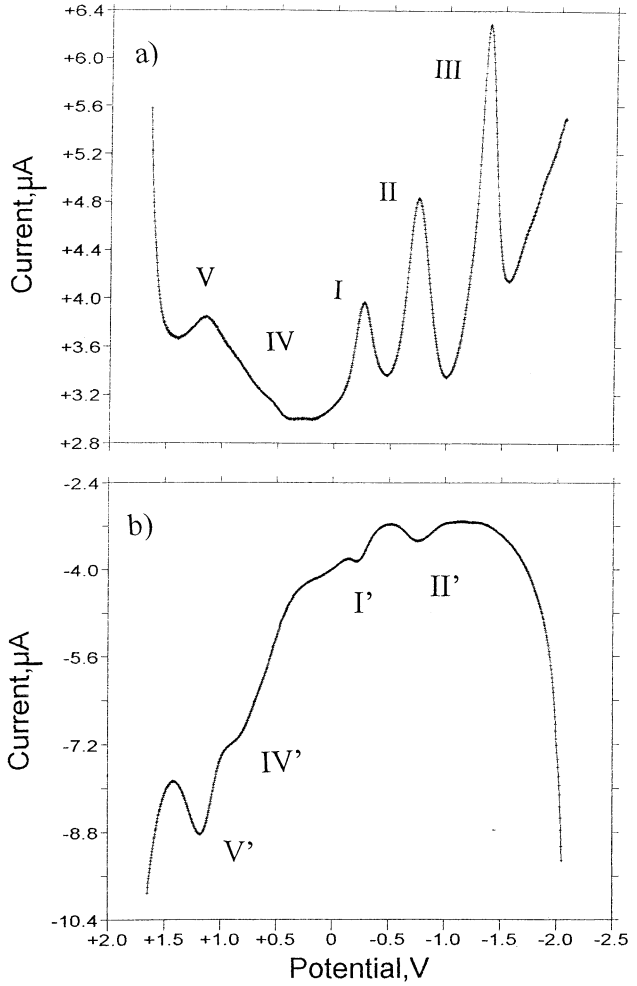

Figure 2. SQWVs at the GCE of a solution of $TTP(BF_4)$ (0.1 mM) in MeCN (0.10 M Et_4NClO_4). (a) Potential scan initiated at +2−0.05 V in the cathodic direction; (b) potential scan initiated at −2.05 V in the anodic direction. Potential step increment 4 mV; SW amplitude 15 mV; frequency 15 Hz.

potential being independent of the frequency in the range from 2 to 200 Hz.

SQWVs provide well-resolved signals as shown in Figure 2. On initiating the potential scan at +1.65 V in the negative direction, broad peaks at +1160 (V) and +850 (IV) appear initially. These correspond to the cathodic counterparts of the oxidation processes V′ and IV′, respectively. At more negative potentials, well-defined peaks are recorded at −250 (I), −735 (II), and −1355 mV (III).

On initiating the potential scan at −2.05 V in the positive direction, weak anodic peaks at −1200 (III′), −775 (II′), and −220 (I′) appear, preceding the main oxidation signal at +1100 mV (V′) overlapped with an ill-defined shoulder (IV′) ca. +850 mV. Similar voltammetric profiles were obtained using 0.10 M Bu_4NPF_6 or 0.10 M $LiClO_4$ as supporting electrolytes in MeCN solution.

3.2. Electrochemistry of TTP@Y in MeCN. The voltammetric profile of TTP@Y-modified electrodes depends on the nature of the supporting electrolyte existing in solution. This can be seen on comparing the SQWV of a 0.1 mM solution of $TTP(BF_4)$ in 0.10 M Et_4NClO_4/MeCN depicted in Figure 3a, with those recorded at TTP@Y-modified electrodes in different MeCN solutions. Thus, SQWVs of TTP@Y recorded in 0.10 M Bu_4NPF_6/MeCN (see Figure 3b) are almost identical to those obtained in solutions of $TTP(BF_4)$. However, SQWVs of

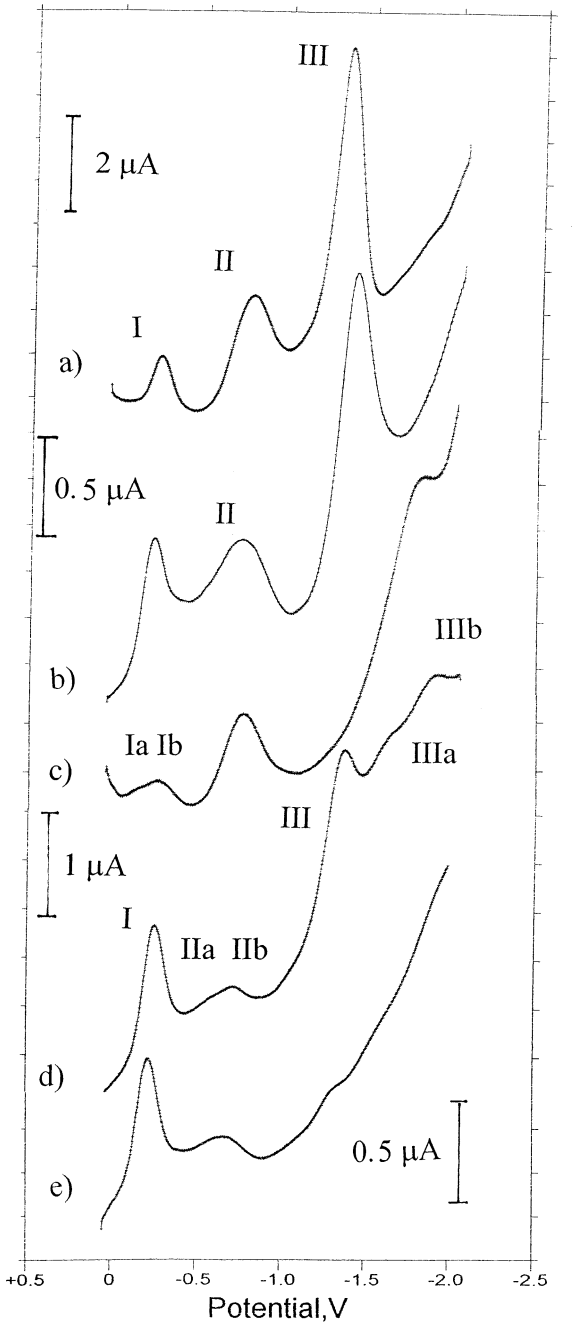

Figure 3. SQWVs of (a) 0.1 mM solution of $TTP(BF_4)$ in 0.10 M Et_4NClO_4 MeCN at an unmodified GCE; (b) TTP@Y-modified electrode in 0.10 M Bu_4NPF_6 MeCN; (c) id. in 0.10 M Et_4NClO_4 MeCN; (d) id. in 0.1 mM $TTP(BF_4)$ plus 0.10 M Et_4NClO_4 MeCN; (e) id. in 0.10 M Et_4NClO_4 plus 0.10 M Bu_4NPF_6 MeCN. Potential scan initiated at +0.05 V in the negative direction. Potential step increment 4 mV; SW amplitude 15 mV; frequency 15 Hz.

TTP@Y-modified electrodes immersed in 0.10 M Et_4NClO_4/MeCN differs significantly from the above voltammograms as depicted in Figure 3c. Here, peak I appears to be resolved into two waves near to −270 and −380 mV, while peak II is slightly displaced toward more negative values (−760 mV), and peak III becomes a broad wave whose peak potential (−1835 mV) is ca. 500 mV more negative than that recorded in $TTP(BF_4)$ solutions.

These data suggest that there are different electrochemical responses for TTP^+ ions in solution phase, and zeolite-associated-TTP^+. In agreement with this idea, SQWVs recorded after immersion of TTP@Y-modified electrodes in a 0.1 mM

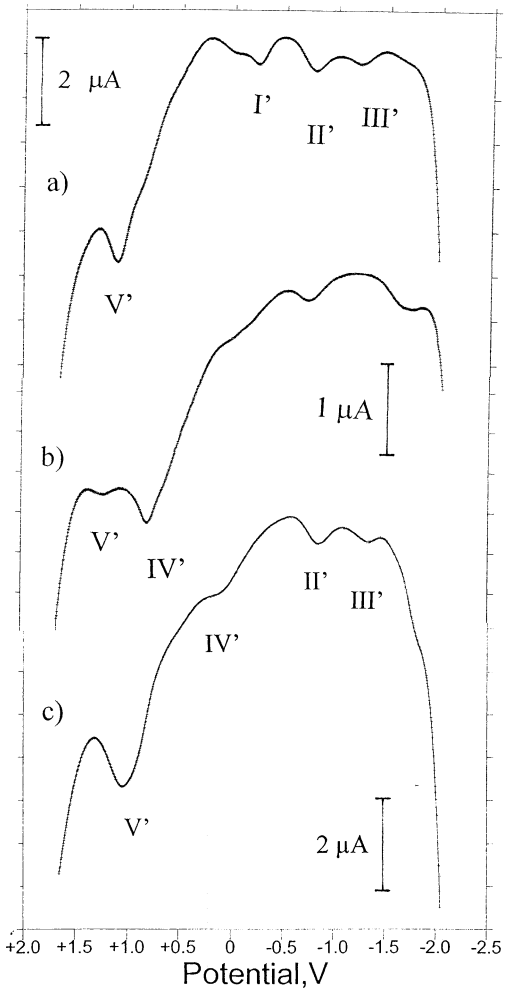

Figure 4. SQWVs of: (a) 0.1 mM solution of $TTP(BF_4)$ in 0.10 M Et_4NClO_4 MeCN at an unmodified GCE; (b) TTP@Y-modified electrode in 0.10 M Et_4NClO_4 MeCN; (c) id. in 0.1 mM $TTP(BF_4)$ plus 0.10 M Et_4NClO_4 MeCN. Potential scan initiated at −2.05 V in the positive direction. Potential step increment 4 mV; SW amplitude 15 mV; frequency 15 Hz.

solution of $TTP(BF_4)$ in 0.10 M Et_4NClO_4/MeCN provide a voltammetric profile in which the signals of "free" and zeolite-associated TTP^+ ions appear to be superimposed. As can be seen in Figure 3d, after the first peak at −235 mV, the second and third signals exhibit a series of overlapped peaks at −670 and −750 mV, and −1360, −1655, and −1920 mV, respectively.

A similar response, apparently resulting from the superposition of independent electrode processes was obtained upon immersion of TTP@Y-modified electrodes in (0.10 M Bu_4NPF_6 + 0.10 M Et_4NClO_4)/MeCN. As shown in Figure 3e, overlapped peaks at −215, −660, −1340, −1650, and −1875 mV appear. Interestingly, in this case, the height of peaks II and III relative to that of peak I is clearly lower than those recorded for $TTP(BF_4)$ in solution.

On scanning the potential anodically, SQWVs of $TTP(BF_4)$ in MeCN solution present a prominent peak at +1100 mV (V) for all $LiClO_4$, Et_4NClO_4, and Bu_4NPF_6 electrolytes whereas the peak at +850 mV (IV) remains ill-defined (see Figure 4a). As can be seen in Figure 4b, at TTP@Y-modified electrodes, peak IV replaces peak V almost entirely. Again, upon immersion of TTP@Y-modified electrodes in 0.1 mM $TTP(BF_4)$ plus 0.10 M Et_4NClO_4 the voltammetric response (see Figure 4c) appears to be a superposition of independent processes, with peaks IV and V well-developed. Upon abrasive treatment of the zeolite probe, the SQWVs of TTP@Y approach those recorded in $TTP(BF_4)$ solutions.

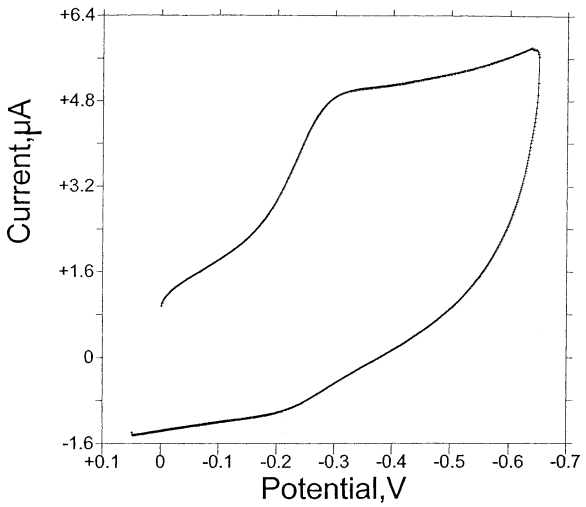

Figure 5. CV of a TTP@Y-modified electrode immersed in MeCN (0.10 M Et_4NClO_4). Potential scan rate 100 mV/s.

On restricting the potential window to the +0.05/−0.65 V range, CVs of PFEs modified by TTP@Y display an apparently single one-electron couple with a formal electrode potential of −255 mV vs SCE, calculated as the half-sum of the cathodic (−325 mV) and anodic (−190 mV) peak potentials (see Figure 5).

The voltammetric response is, as previously noted, strongly conditioned by the nature of the supporting electrolyte. Thus, as shown in Figure 6a,b, SQWVs of TTP@Y in 0.10 M Bu_4NPF_6 are identical to those recorded in solutions of $TTP(BF_4)$ in the same medium. In contrast, in $LiClO_4$ and Et_4NClO_4 electrolytes, SQWVs of TTP@Y differ from those of $TTP(BF_4)$ in solution. As shown in Figure 6c,*d*, while TTP^+ in solution presents only one well-defined peak at −250 mV (Ia), TTP@Y-modified electrodes exhibit two overlapped peaks at −280 (Ib) and −385 mV (Ic) in Et_4NClO_4/MeCN and $LiClO_4$/MeCN. Furthermore, the SQWVs of TTP@Y in Et_4NClO_4 and $LiClO_4$ electrolytes show peak currents 5−10 times larger than those recorded for such electrodes immersed in Bu_4NPF_6 ones. Remarkably, the peak potentials of peaks Ib and Ic differ 25−50 mV from one electrolyte to another and are shifted toward more negative values on increasing the concentration of supporting electrolyte.

Blank CV and SQWV experiments performed on the electrolyte solution remaining after repeated experiments on TTP@Y-modified electrodes do not provide voltammetric peaks, suggesting that no significant leaching takes place under these experimental conditions.

3.3. Electrochemistry of $TTP(BF_4)$ in Aqueous Media. Since $TTP(BF_4)$ was insoluble in aqueous media, the electrochemical response of that solid attached to glassy carbon, platinum, and gold electrodes was studied following the "voltammetry of microparticles" approach.[40] Well-defined responses were obtained in the potential range from 0.0 to −0.65 V, as illustrated in Figure 7a,b, in which the CVs for lightly ground and abrasive-conditioned $TTP(BF_4)$ attached to a GCE electrode and immersed in 1.0 M $NaNO_3$ are presented. In the first case the cathodic region exhibits only one well-defined peak at −300 mV (I). whereas in the anodic region its anodic counterpart I′ is followed by a second oxidation peak (VI′) near to 0 mV. Under abrasive conditioning of the $TTP(BF_4)$-modified

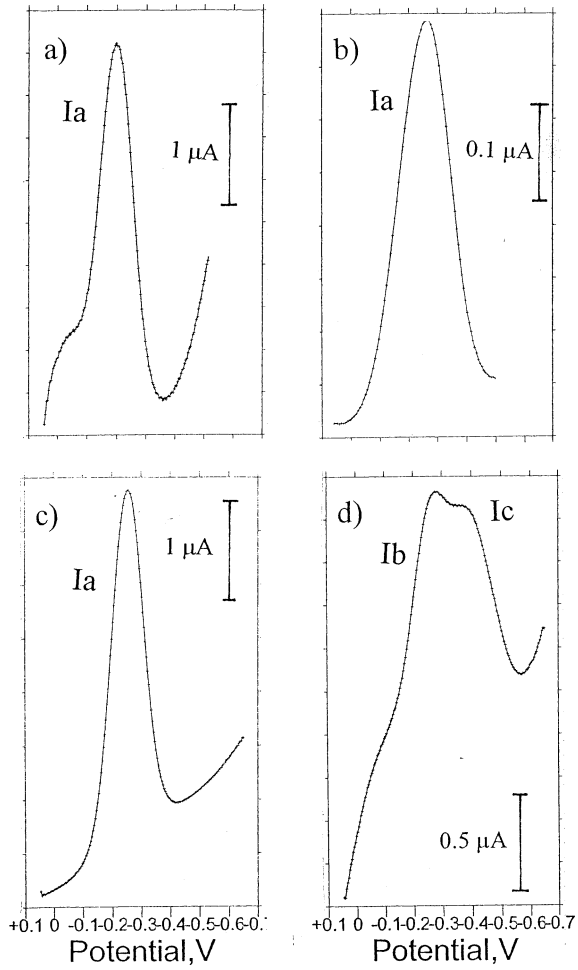

Figure 6. SQWVs of a (a) 0.20 mM solution of $TTP(BF_4)$ in 0.10 M Bu_4NPF_6 MeCN; (b) TTP@Y-modified electrode in 0.10 M Bu_4NPF_6 MeCN; (c) 0.20 mM solution of $TTP(BF_4)$ in 0.10 M Et_4NClO_4 MeCN; (d) TTP@Y-modified electrode in 0.10 M Et_4NClO_4 MeCN. Potential step increment 4 mV; SW amplitude 15 mV; frequency 15 Hz.

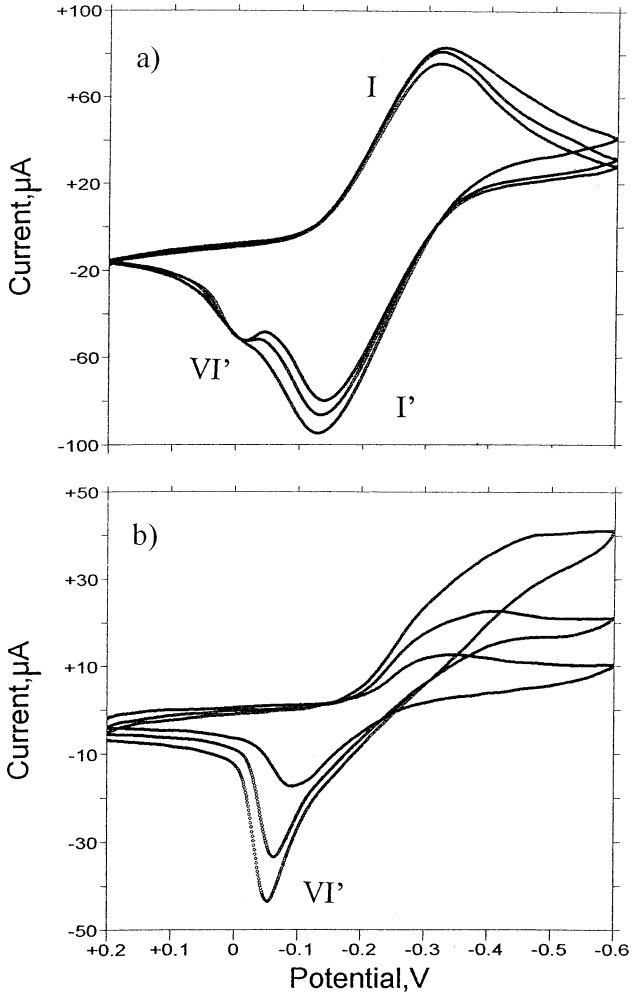

Figure 7. CVs of (a) $TTP(BF_4)$-modified electrode immersed in water (1.0 M $NaNO_3$); (b) abrasive-conditioned $TTP(BF_4)$ electrode immersed in water (1.0 M $NaNO_3$). Potential scan rate 50 mV/s.

electrode, peak VI′ is enhanced at the expense of peak I′ and an ill-defined shoulder near −400 mV (VI) follows the initial reduction step I.

Upon repetitive cycling the potential scan, peaks VI/VI′ are considerably enhanced denoting that accumulation of electroactive species on the electrode surface takes place. Peaks VI and VI′ present a symmetric, Gaussian-like profile while their peak currents become proportional to the potential scan rate. These are characteristics properties of voltammograms of surface-confined species, suggesting that adsorption on the electrode surface occurs.[42]

To confirm this possibility, a series of electrodes were prepared by soaking during 30 s bare glassy carbon, platinum, and gold electrodes in a diluted (0.20 mM) solution of $TTP(BF_4)$ in MeCN. The electrodes were further washed and transferred to aqueous electrolytes to record CVs. As shown in Figure 8a for Pt and 8b for Au electrodes, only peaks VI/VI′ appear in multiple scan CVs. An identical response was obtained for TTP^+ adsorbed on glassy carbon electrodes.

In agreement with CV data, in the first scan of SQWVs recorded at $TTP(BF_4)$-modified electrodes only peak I is recorded at square wave frequencies below 25 Hz, as can be seen in Figure 9a. For frequencies larger than 25 Hz, peak VI also appears in the initial SQWVs of $TTP(BF_4)$-modified electrodes (see Figure 9b,c). After a few scans, only peak VI remains, the peak current being proportional to the square wave frequency. Similar results were obtained for TTP^+ adsorbed on glassy carbon, Pt, and Au electrodes.

3.4. Electrochemistry of TTP@Y in Aqueous Media. CVs of TTP@Y-modified electrodes immersed in aqueous electrolytes do not present well-defined peaks in the +1.25 to −1.45 V potential range (se Figure 10a). In the region of potentials between 0.0 and −0.65 V, only one well-defined couple appears in the initial scan voltammograms as can be seen in Figure 10b. Upon repetitive cycling the potential scan, the voltammograms become ill-defined while the peak current for both cathodic and anodic peaks decreases slowly. No additional peaks were detected in repetitive voltammetry; in particular, processes VI and VI′ are entirely absent (see Figure 10b). As obtained for TTP@Y-modified electrodes in MeCN, after repeated experiments on each one of the modified electrodes immersed in aqueous electrolytes, the remaining solution becomes electrochemically silent on CVs at the bare GCE.

The amount of electroactive TTP^+ ions in TTP@Y was estimated from the quantities of charge passed upon integration of the area under voltammetric peaks. For the electrode coverages used here (typically 4 mg/cm^2 of zeolite surface density) and lightly ground conditioning of samples, the net quantity of charge passed was 0.25 μC. Since the total TTP^+ concentration in the zeolite was 1.6×10^{-7} mol/mg, one can estimate that only 0.6% of zeolite-associated TTP^+ is electroactive under our experimental conditions.

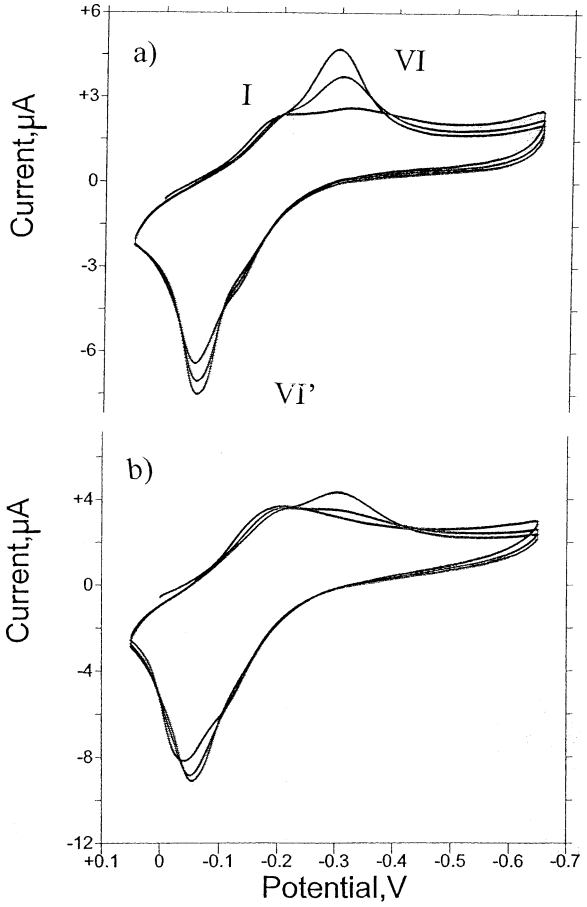

Figure 8. CVs of (a) TTP^+ adsorbed on Pt; (b) TTP^+ adsorbed on Au, both immersed in 0.20 M $LiNO_3$. Potential scan rate 100 mV/s.

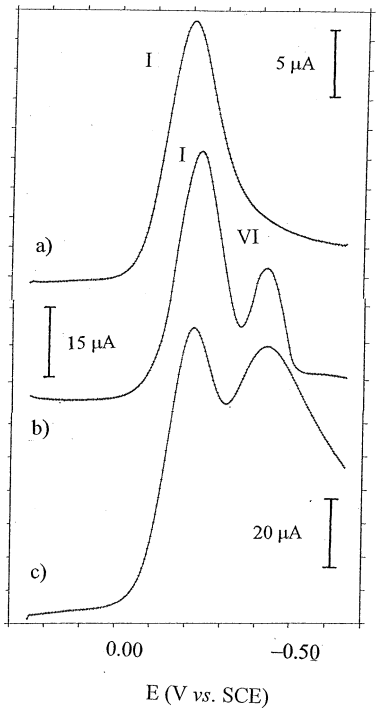

Figure 9. First scan SQWVs of a $TTP(BF_4)$-modified electrode immersed in water (1.0 M $NaNO_3$). Potential step increment 4 mV; square wave amplitude 15 mV; frequency: (a) 15 Hz; (b) 50 Hz; (c) 100 Hz.

SQWVs of TTP@Y-modified electrodes changes remarkably on repetitive scan experiments. As can be seen in Figure 11, an

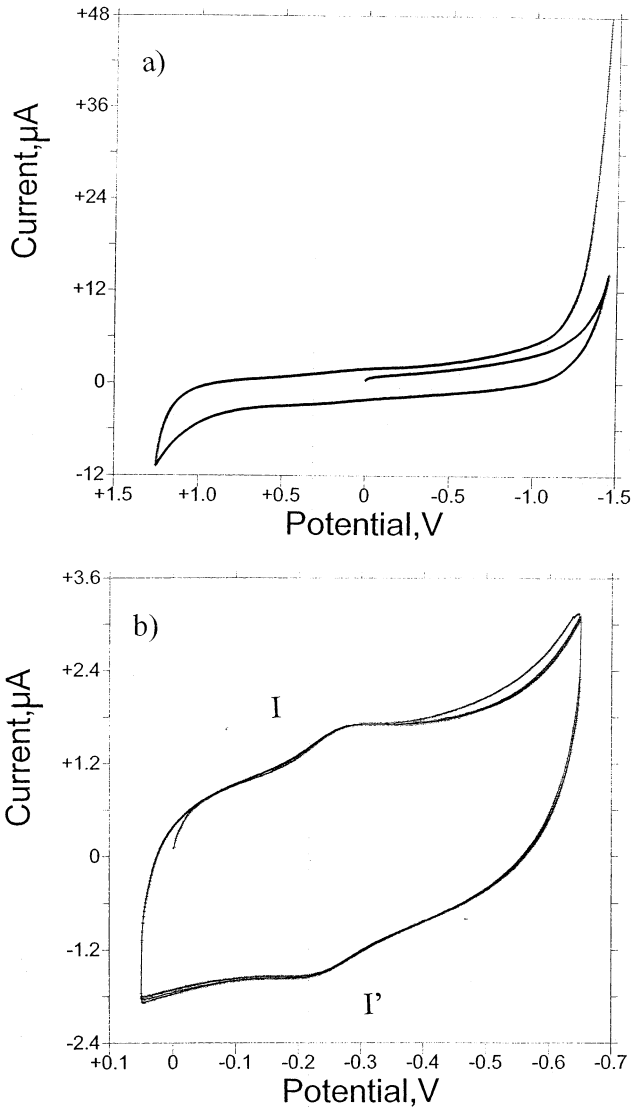

Figure 10. CV of a TTP@Y-modified electrode immersed in 0.10 M $NaNO_3$. (a) +1.25/−1.45 V potential range; (b) +0.05/−0.65 V potential range. Potential scan rate 100 mV/s.

isolated cathodic peak at −325 mV (Ia) appears in the first scan; however, upon repeating the SQWV the peak is shifted toward more negative potentials, ca. −400 mV (peak Ic), and is accompanied by a peak near −280 mV (Ib) whose height increases progressively in successive scans. Once several scans have been performed the electrochemical response becomes essentially stationary but remarkably frequency-dependent. As can be seen in Figure 12, after several (3−6) scans, only peak Ic is recorded at square wave frequencies larger than 25 Hz, whereas for frequencies below 5 Hz, only peak Ib appears. Consistently, for intermediate square wave frequencies, both peaks Ib and Ic coexist in SQWVs. This two-peak response is also obtained on decreasing the potential step increment at low frequencies.

For our purposes, the relevant point to emphasize is that in aqueous electrolytes TTP^+ ions display an electrochemical response that differs significantly from that obtained at TTP@Y-modified electrodes. Apart from the differences in the peak potential values for peaks Ia, Ib, Ic, and VI, some relevant differences have been obtained. Thus, (a) in first scan voltammograms, $TTP(BF_4)$ electrodes exhibit both peaks Ia and VI at relatively large frequencies (see Figure 9), while for TTP@Y only peak Ia appears at all frequencies; (b) on repetitive SQWV,

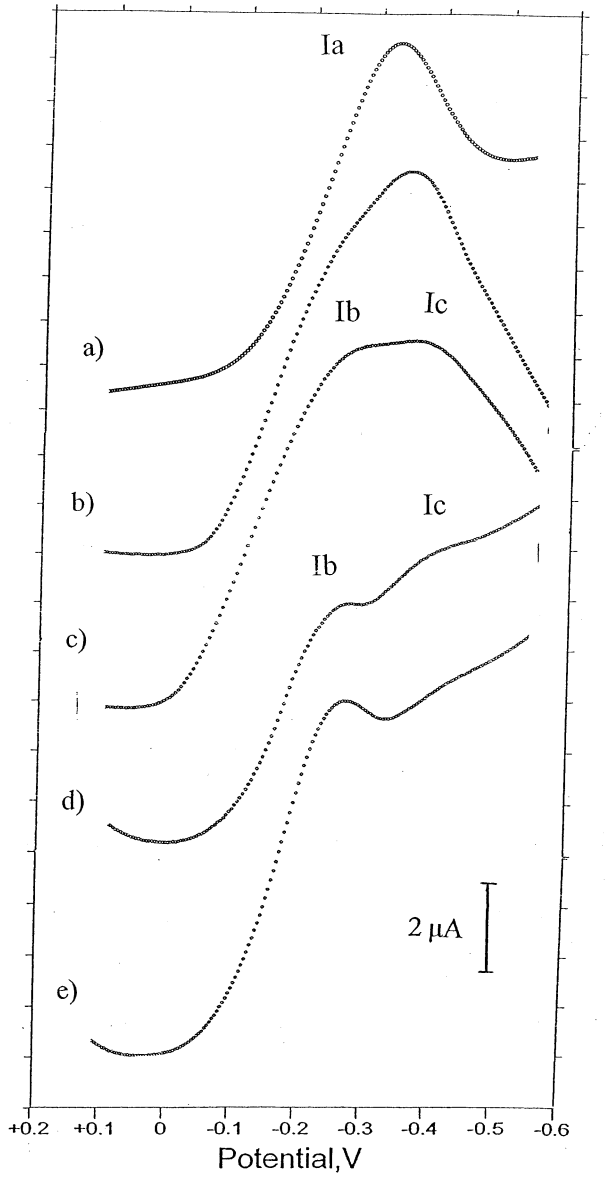

Figure 11. Successive SQWVs performed on a TTP@Y-modified electrode in 0.10 M $LiNO_3$. Scan number: (a) 1; (b) 2; (c) 3; (d) 7; (e) 10. Potential step increment 4 mV; SW amplitude 15 mV; frequency 15 Hz.

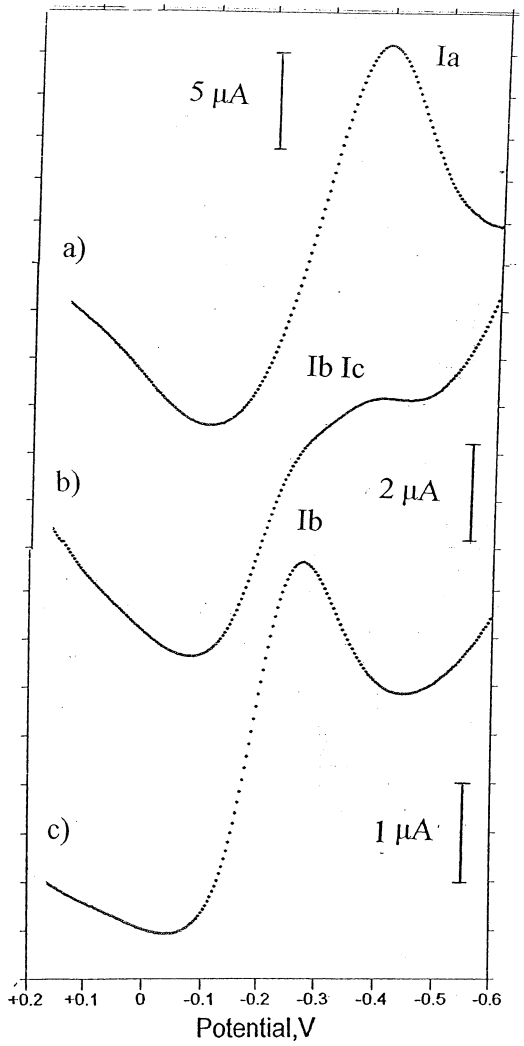

Figure 12. SQWVs of a TTP@Y-modified electrode in 0.10 M $NaNO_3$ recorded after 5 scans. (a) $f = 100$ Hz; (b) $f = 15$ Hz; (c) $f = 5$ Hz. In all experiments the potential step increment was 4 mV and the SW amplitude 15 mV.

only peak VI remains at the entire range of frequencies for TTP-(BF_4) electrodes, while for TTP@Y peak Ic replaces entirely peak Ib at large f values, while only peak Ib appears at low frequencies (see Figure 12).

To analyze this electrochemical response in more detail, we have studied the variation of the peak potential, E_p, peak half-width, $W_{1/2}$, and peak current, Δi_p, with the square wave frequency for electrode processes Ia, Ib, Ic, and VI. First of all, the response for TTP^+ in MeCN solution (peak Ia) fits to a reversible one-electron transfer; the peak potential (data points A in Figure 13) is independent of the frequency as well as the peak half-width whose value (130 mV, see data A in the inset of Figure 13) approaches the theoretical value (126 mV) for such a reversible case.[38]

The above response differs from that of TTP(BF_4) attached to carbon, platinum, or gold electrodes in which the peak potential of the initial reduction process (in first scan SQWVs) is negatively shifted on increasing the frequency. A linear dependence of E_p on log f, illustrated in Figure 13 (data points B), was obtained. The slope of such representation is 30 mV/decade as expected for a one-electron transfer followed by a chemical reaction.[43] In agreement with this scheme, $W_{1/2}$ (points B in the inset in Figure 13) varies with the square wave frequency.

Such responses contrast with those of peaks Ib and Ic recorded in TTP@Y-modified electrodes after a few scans. As illustrated in points C in Figure 13, peak potentials of both peaks remain essentially frequency-independent, suggesting a reversible behavior. Their peak half-widths estimated after background current subtraction (210 mV) are also f-independent but larger than those expected for a reversible one-electron transfer.

On studying the variation of the peak current, Δi_p, on the frequency, one obtains significant differences between the electrode processes observed at TTP@Y-modified electrodes and those at TTP(BF_4). Thus, for initial SQWVs of TTP@Y, the peak current is proportional to the square root of the frequency (data points A in Figure 14). In contrast, for TTP-(BF_4)-modified electrodes, at low frequencies Δi_p varies almost linearly with $f^{1/2}$ but the peak current tends to a limiting value at high f values (data points B in Figure 14). This variation can in principle be explained on assuming that the dissolution of sparingly soluble TTP(BF_4) acts as a rate-determining step of

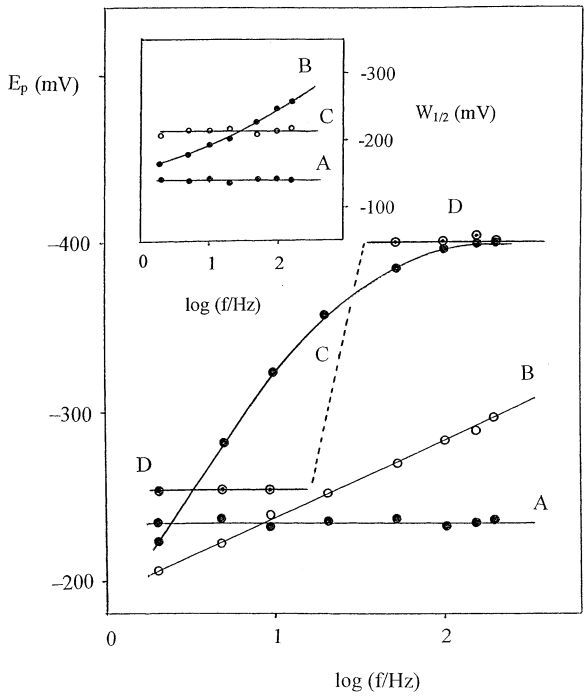

Figure 13. Variation of E_p and $W_{1/2}$ (inset) on log f in SQWVs (potential step 4 mV; SW amplitude 15 mV). A: 0.20 mM solution of $TTP(BF_4)$ in MeCN (0.10 M Et_4NClO_4); B: solid $TTP(BF_4)$ attached to a GCE immersed in 0.10 M $NaNO_3$; C: first scan in freshly prepared TTP@Y-modified electrodes immersed in 0.10 M $NaNO_3$ (peak Ia); D: peaks Ib and Ic recorded after 5 scans in a TTP@Y-modified electrode immersed in 0.10 M $NaNO_3$.

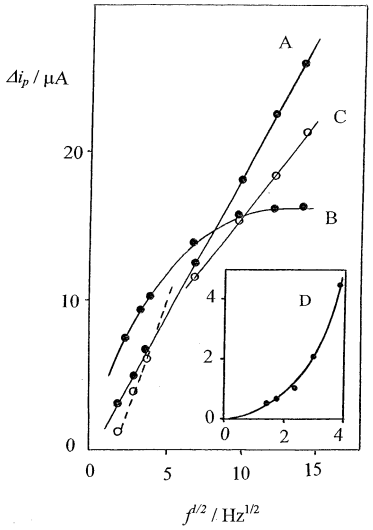

Figure 14. Plots of Δi_p vs $f^{1/2}$ in SQWVs (potential step 4 mV; SW amplitude 15 mV). A: 0.20 mM solution of $TTP(BF_4)$ in MeCN (0.10 M Et_4NClO_4); B: solid $TTP(BF_4)$ attached to a GCE immersed in 0.10 M $NaNO_3$; C: first scan in freshly prepared TTP@Y-modified electrodes immersed in 0.10 M $NaNO_3$ (peak Ia); D: peak Ib recorded after 5 scans in a TTP@Y-modified electrode immersed in 0.10 M $NaNO_3$.

the overall electrode process, the slow dissolution of $TTP(BF_4)$ limiting the flux of "free" TTP^+ ions toward the electrode surface.

The variation of the response of TTP@Y-modified electrodes from the first to the subsequent scans can also be seen in Figure 14. In first scan SQWVs recorded on freshly prepared TTP@Y-modified electrodes (points C), the peak current of Ia varies linearly with $f^{1/2}$ at relatively high frequencies, but there is a discontinuity with peak currents measured at low frequencies. After repeated experiments on the same modified electrode, Δi_p values for peak Ic remain linearly dependent on $f^{1/2}$, suggesting a diffusive control of such electrochemical process. However, for peak Ib (see points D in the inset in Figure 14), the peak current approaches the proportionality with the frequency, as expected for electroactive species immobilized on the electrode surface.[44]

TABLE 1: Temperature Dependence of Peak Potentials for Processes Ib and Ic in SQWVs of TTP@Y-Modified Electrodes Immersed in Different Aqueous Media[a]

	Ep (mV vs SCE)					
	0.20 M $LiNO_3$		0.20 M $NaNO_3$		0.20 M KNO_3	
T (K)	Ib	Ic	Ib	Ic	Ib	Ic
278	−280	−410	−265	−400	−310	−450
285	−275	−405	−260	−395	−300	−435
298	−265	−400	−250	−380	−280	−405
313	−250	−390	−240	−365	−260	−370
327	−235	−385	−225	−350	−240	−340
338	−225	−380	−220	−340	−225	−310

[a] SQWVs obtained at PFEs after 5 scans. Potential step 4 MV; SW amplitude 15 MV. SQW frequency 5 Hz for Ib and 25 Hz for Ic.

The differences between the studied electrode processes are also illustrated by the variation of peak potentials on the square wave amplitude, E_{SW}. For SQWVs at relatively high frequencies, both peaks I and VI appear in the first scan recorded at $TTP(BF_4)$-modified electrodes. On increasing E_{SW}, peak VI is enhanced whereas peak Ia decreases very slowly. For TTP@Y-modified electrodes, only peak Ic appears, the peak potential being E_{SW}-independent. On the contrary, the peak potentials of all the recorded processes remain essentially constant upon variations of the potential step increment, ΔE.

As observed in contact with MeCN, peak potentials for processes Ib and Ic recorded in aqueous media for TTP@Y-modified electrodes differs slightly from one electrolyte to another and are negatively shifted on increasing the concentration of supporting electrolyte. On increasing temperature, peak potentials of Ib and Ic becomes more negative, with linear dependences of E_p on T. The obtained data are summarized in Table 1.

4. Discussion

Electrochemical data indicate that the electrode process Ia/Ia′ obtained for $TTP(BF_4)$ in MeCN solution can be represented as a one-electron reversible diffusion-controlled process:

$$TTP^+(s) + e^- = TTP(s) \qquad (1)$$

where (s) denotes species in solution. This in principle single behavior contrasts with that described for pyrylium ions in large time scale experiments in aprotic solvents, in which pyrylium ions are reduced to bipyranylidene together with pyrane through a process kinetically controlled by the irreversible dimerization of the radicals formed after the initial electron-transfer step.[45,46]

Reduction processes II and III must correspond to the reduction of the aromatic thiopyrylium and phenyl systems. In aprotic solvents, aromatic hydrocarbons show two reversible one-electron cathodic waves to give, successively, a radical anion and a dianion.[47] The observed response can be conditioned, however, by the presence of protonated impurities or by proton-transfer processes with the solvent.[48,49] Accordingly, processes II and III can in principle be represented as two successive one-electron-transfer processes:

$$TTP(s) + e^- = TTP^-(s) \quad (2)$$

$$TTP^-(s) + e^- = TTP^{2-}(s) \quad (3)$$

At potentials near to +1.0 V, the aromatic thiopyrylium and phenyl rings are presumably oxidized to cationic species following the scheme described for thianthrene and anthracene:[50−52]

$$TTP^+(s) = TTP^{2+}(s) + e^- \quad (4)$$

Electrochemical oxidation of aromatic systems such as anthracene or thianthrene takes place in two consecutive one-electron-transfer processes with formation of a radical cation and a dication.[50] However, nucleophilic agents such as MeCN[51] or water[52] can react with the generated cationic species, then producing a relatively complicated electrochemicay response.

With regard to the electrochemistry of zeolite-asociated species, the question is to elucidate if the electrode processes observed for TTP@Y can be represented as a single electron-transfer between electroactive species attached to the zeolite boundary, or only a purely extrazeolitic mechanism is operative. In both cases, the electron-transfer process has to be accompanied by the ingress of a charge-compensating ion, M^+, from the solution to the zeolite channel system.[3,4] Thus, the extrazeolitic electrochemical process can be described for TTP^+ as a two-step process:

$$TTP^+(b) + M^+(s) = TTP^+(s) + M^+(b) \quad (5)$$

$$TTP^+(s) + e^- = TTP(s) \quad (6)$$

where (b) denotes the zeolite boundary and (s) species in solution. The boundary-asociated process can be represented as

$$TTP^+(b) + M^+(s) + e^- = TTP(b) + M^+(b) \quad (7)$$

To study in detail this problem, it is pertinent to analyze the influence of the supporting electrolyte in the electrochemistry of TTP@Y-modified electrodes. Thus, it should be noted that the electrochemical response of TTP@Y-modified electrodes is considerably lowered in Bu_4NPF_6/MeCN with respect to those obtained in Et_4NClO_4/MeCN and $LiClO_4$/MeCN electrolytes. Although Li^+ and Et_4N^+ cations can enter in the zeolite pore systems,[53] the Bu_4N^+ cation is essentially size-excluded from the zeolite-Y cage and pore system.[6] Thus, the electroactivity observed in Bu_4NPF_6/MeCN (peak Ia) can be attributed essentially to "extrazeolite" TTP^+ ions adsorbed or occluded in the external surfaces of the zeolite particles.[13] In Et_4NClO_4/MeCN and $LiClO_4$/MeCN electrolytes, peak Ia is replaced in repetitive voltammetry by peaks Ib and Ic, attributable to zeolite-associated species, suggesting that electron-transfer processes coupled with the ingress of electrolyte countercations are operative in addition to the reduction of "extrazeolite" TTP^+ ions. This is in agreement with (see Figures 3, 4, and 6) the following: (i) the significant difference between the voltammetric profiles of TTP^+ in solution and TTP@Y for processes III−IV and V−VI; (ii) the observation of overlapped peaks upon immersion of TTP@Y-modified electrodes in Bu_4NPF_6 + Et_4NClO_4 electrolytes; (iii) the observation of overlapped peaks upon immersion of TTP@Y-modified electrodes in $TTP(BF_4)$ solutions in Et_4NClO_4 electrolytes; and (iv) the observed variation of peak potentials with the concentration of supporting electrolyte.

In both the schemes described by eqs 5,6 and also eq 7, the extent of multielectron transfer processes to zeolite-associated species must be limited by the rate of exchange of multiple electrolyte cations. Consistent with those considerations, the height of peaks II and III relative to that of peak I for TTP@Y is considerably decreased (see Figure 3) with respect to that in solutions of $TTP(BF_4)$ while peak III is displaced in TTP@Y to a potential ca. 500 mV more negative than in $TTP(BF_4)$ solutions.

Oxidation processes leading to the formation of positively charged species are probably favored in zeolite-associated systems. As observed in reduction processes, the profile of peaks IV′ and V′ in SQWVs of TTP@Y in Bu_4NPF_6 equals that in $TTP(BF_4)$ solutions in all electrolytes, but differs from those obtained in Et_4NClO_4/MeCN and $LiClO_4$/MeCN. These observations suggest that zeolite-associated species are involved in such electrochemical response. The electron-transfer process must involve the issue of charge-compensating cations through an extrazeolitic mechanism:

$$TTP^+(b) + M^+(b) = TTP^+(s) + M^+(s) \quad (8)$$

$$TTP^+(s) = TTP^{2+}(s) + e^- \quad (9)$$

or a boundary-asssociated pathway:

$$TTP^+(b) + M^+(b) = TTP^{2+}(b) + M^+(s) + e^- \quad (10)$$

The electrochemical response of $TTP(BF_4)$-modified electrodes in contact with aqueous electrolytes is more complicated, with "adsorptive" processes VI and VI′ replacing the initial reduction step I in repetitive voltammetry. The large separation between the peak potentials of processes VI and VI′ suggests that the reduction process is followed by a chemical reaction leading to an oxidized species whose subsequent reduction yields TTP^+ adsorbed on the electrode surface. It is known that in protic solvents pyrylium ions yields a one-electron reduction followed by dimerization to dipyran.[54] Following this scheme, the initial reduction process (peak Ia recorded in initial scans) of TTP^+ yields a reactive species which rapidly forms a deposit of neutral dithiopyran $(TTP)_2$ on the electrode surface. In anodic scans, this is oxidized (process VI′) to adsorbed TTP^+, and subsequently reduced (process VI) to surface-confined $(TTP)_2$.

Organic molecules having aromatic π-electron systems or containing thiol, nitro, carbonyl, or nitrile groups are able to adsorb on electrode surfaces. Adsorption may involve electrostatic (such as ion−dipole) interactions, but also chemical bonds between certain electrode materials and substrates are possible.[55] The limiting surface coverage is controlled by the cross-sectional area of the adsorbed molecule, which, in turn, is dependent upon the orientation at which it is bonded to the surface. In view of the recognized affinity of gold surfaces for S-containing groups,[55] the fact that the electrochemical behavior was identical for glassy carbon, Pt and Au electrodes suggests that there is no place for an adsorption through the S atom of TTP^+. Accordingly, one can expect that a flat orientational state, similar to that described for the benzoquinone/1,4-dihydroxybenzene system on Pt, can be operative.[42] As in this system, the electrochemical response of adsorbed species differs from the reversible behavior observed in solution, suggesting that a relatively strong adsorption occurs.[56]

The electrochemical response of TTP@Y-modified electrodes immersed in aqueous media differs from that previously discussed for $TTP(BF_4)$. In repetitive SQWVs at TTP@Y-modified electrodes, peaks Ib appearing at low frequencies and

having a thin-layer behavior, and Ic, appearing at high frequencies with a thick-layer response, replace the initial solution-like process Ia. For $TTP(BF_4)$, peak VI, which exhibits a typical "adsorptive" behavior, replaces entirely the initial diffusive response Ia in repetitive experiments at all frequencies. It should be noted that peaks VI and VI′ are absent at TTP@Y-modified electrodes under repetitive voltammetric conditions. Only a weak VI′ signal appears upon abrasive conditioning of the zeolite sample in repetitive experiments. This is in contrast with the results reported by Hui and Baker for Y zeolite-associated methyl viologen,[17] for which a clear "adsorptive" response was found. Possible differences can result from the different conditioning of the zeolite-modified electrodes.

The presence of two different potential scan rate dependencies in TTP@Y-modified electrodes suggests that both "thick-layer" diffusion-controlled (Δi_p proportional to $f^{1/2}$, peak Ic) and "thin-layer" interface-confined processes (Δi_p proportional to f, peak Ib) occur. The surface reactions occur in the thin-film mode when diffusion of electrolyte cations within the zeolite channels and cages is not rate-determining. A similar dual behavior has been reported for redox and conducting polymer films[57] and some nonconducting microcrystalline complexes immersed in aqueous electrolytes.[58] The observation of a stable response on repetitive voltammetries can be considered, following Bessel and Rolison, as a characteristic of possible electrochemical processes involving boundary-associated electroactive species.[26]

Following Turro and García-Garibay,[28] topological redox isomers in zeolites may be (i) entirely external; (ii) bound to the external surface topology (or boundary) of the zeolite (including size-excluded and adsorbed/occluded in defect sites and/or truncated or partially broken zeolite supercages, and encapsulated in the first layer of complete supercages of the zeolite's outermost boundary); (iii) adsorbed into the inside of the zeolite crystal but free to sample the global pore lattice topology; (iv) size-included in the interior of the zeolite (within a supercage, channel intersection, or sodalite cage).

The electrochemistry of TTP@Y can be rationalized on the basis of the superposition of the responses of at least three topological redox isomers: (a) TTP^+ ions adsorbed or occluded in the external surface layer of the zeolite particles passing to the solution by leaching without need of the interchange of charge-compensating electrolyte cations; (b) TTP^+ ions weakly attached to the zeolite boundary that produce a thick-layer response controlled by the diffusion of electrolyte cations and/or TTP^+ ions through the zeolite channels; and (c) TTP^+ ions more strongly attached to the zeolite boundary responsible for a thin-layer behavior, in which, as previously described for Y zeolite-associated $Mn(salen)N_3$,[29] the diffusion of electrolyte countercations through the zeolite system does not enter as the rate-determining step.

From this view, the isomer (a), identical to that of TTP^+ ions in solution, must be responsible for the weak electrochemistry observed for TTP@Y in Bu_4N^+/MeCN and contributes significantly to the response obtained during the initial scan voltammograms in all other electrolytes (process Ia). The response of boundary-associated isomers (b) and (c) prevails after a few potential scans and the electron transfer is conditioned by the ingress of non size-excluded electrolyte cations (Li^+, Na^+, K^+, Et_4N^+) into the zeolite channels.

Tentatively, it appears reasonable to associate the thick-layer behavior (peak Ic) to a topological redox isomer adsorbed/occluded in defect sites of the external boundary of the zeolite particles. In this scheme, the thin-layer response (peak Ib) can be associated with TTP^+ ions located in truncated or partially broken zeolite supercages.

TABLE 2: Formal Electrode Potentials, Free Energy, Enthalpy, and Entropy Calculated for Electrochemicall Processes Ia and Ib from Peak Potentials in SQWVs at Temperatures Ranging from 273 to 338 K in Different Aqueous Electrolytes All in Concentration 0.20 M[a]

	TTP@Y		TP@Y	
electrolyte	Ib	Ic	Ib	Ic
		$\Delta G°$ (kJ/mol)		
$LiNO_3$	+1.2(5)	+14.8(5)	+2.2(5)	+13.3(5)
$NaNO_3$	−0.7(4)	+12.3(5)	+0.8(4)	+13.3(5)
KNO_3	+1.7(4)	+15.2(5)	+3.7(5)	+15.7(5)
		$\Delta H°$ (kJ/mol)		
$LiNO_3$	+37(4)	+41(5)	+28(4)	+30(5)
$NaNO_3$	+18(3)	+44(5)	+23(4)	+42(5)
KNO_3	+61(6)	+53(5)	+44(5)	+82(7)
		$\Delta S°$ (J/mol K)		
$LiNO_3$	+119(8)	+90(6)	+90(5)	+48(3)
$NaNO_3$	+63(4)	+108(6)	+74(5)	+98(6)
KNO_3	+199(9)	+128(7)	+137(8)	+223(9)

[a] SQWVs obtained at PFEs after 5 scans. Potential step 4 MV; SW amplitude l15 mv. SQW frequency 5 Hz for Ib and 25 Hz for Ic. Numbers in parenthesis represent the estimated uncertainty in the last significant figure.

It should be noted, however, that the voltammetric response of boundary-associated isomers (b) and (c) can in principle be described either by the 'extrazeolitic' scheme represented by Eqs. (3)−(4) and by the 'boundary-associated' path described by eq 5. The absence of adsorption effects for TTP@Y in contact with aqueous electrolytes, however, appears to be in agreement with a boundary-associated mechanism.

Variations of peak potentials of Ib and Ic on temperature provided linear representations from which thermochemical parameters can be estimated for the overall electrode process represented by eq 6, as described for zeolite-associated $Mn(salen)N_3$.[29] The values obtained for TP@Y and TTP@Y in aqueous $LiNO_3$, $NaNO_3$, and KNO_3 electrolytes are summarized in Table 2. In this table the free energy values have been calculated from the peak potentials in SQWVs recorded after 5 scans at 5 Hz (peak Ib) and 25 Hz (peak Ic) assuming that the peak potentials are identical to formal electrode potentials, as is applied to reversible processes in SQWV.[42] For both TP@Y and TTP@Y, systems in both Ib and Ic peaks, it can be seen that $\Delta G°$, $\Delta H°$, and $\Delta S°$ vary from one electrolyte to another. Interestingly enough, $\Delta G°$ values are in the order $Na^+ < Li^+ < K^+$ for both Ib and Ic peaks and for both TP@Y and TTP@Y systems. This must result from the difference in the energy of the transfer of the electrolyte countercation from the solution phase to the zeolite system.[29] Roughly speaking, these differences may reflect a compromise between the cation mobility derived from hydrated radii, which following Calzaferri et al.,[22] increases in the order $Li^+ < Na^+ < K^+$, and the theoretical mobility of the desolvated cations ($Li^+ > Na^+ > K^+$).

Consistent with the thermochemical cycle proposed for this kind of systems,[29] the differences between the $\Delta G°$ values calculated for each pair of electrolytes are quite similar for TP@Y and TTP@Y. Thus, $\Delta G°(Li^+) - \Delta G°(Na^+)$ is consistently close to $+1.9 \pm 0.5$ kJ/mol while $\Delta G°(Na^+) - \Delta G°(K^+)$ is equal to -2.4 ± 0.5 kJ/mol for peaks Ib and Ic in both TP@Y and TTP@Y systems.

Finally, the difference in the value of $\Delta G°$ for topological redox isomers responsible for electrode processes Ib and Ic reflects their relative stability with regard to their transfer from the solution to the zeolite boundary. On comparing the $\Delta G°$

values in Table 1, one finds that the difference $\Delta G°$(Ib) − $\Delta G°$(Ic) is consistently near −13 ± 2 kJ/mol for TP@Y and TTP@Y. This result is in principle in agreement with the idea that two different boundary-associated topological redox isomers exist, having a site-characteristic energy of attachment. Peak potential differences have been reported for electroactive ions having different coordinative arrangement in solid microparticles attached to inert electrodes.[40]

5. Final Considerations

The voltammetry of zeolite-asssociated TTP^+ ions exhibit some subtle differences from that of pyrylium ions in solution. In contact with MeCN containing size-excluded Bu_4N^+ ions the electrochemistry of TTP@Y is identical to that of TTP(BF_4) in solution. However, in the presence of Li^+/MeCN and Et_4N^+/MeCN electrolytes, the response of TTP@Y differs from that of TTP^+ in solution phase, suggesting that the electrochemical response of zeolite-asociated species coupled with the ingress of electrolyte cations in the zeolite is superimposed to that of TTP^+ ions occluded or retained in the external zeolite surface.

On repetitive square wave voltammetry, a strongly frequency-dependent dual response consisting of thin-layer and thick-layer modes was obtained for TTP@Y-modified electrodes. This can be associated with the presence of different topological redox isomers bound to the external boundary layer of the zeolite particles. Although further research is needed to properly elucidate the nature of the electrochemical processes involving zeolite-associated species, the absence of adsorption effects in TTP@Y-modified electrodes, in contrast with those observed in TTP(BF_4)-modified electrodes appears to be consistent with a boundary-associated pathway.

References and Notes

(1) Rolison, D. R. *Chem. Rev.* **1990**, *90*, 867.
(2) Walcarius, A.; Wang, J. *J. Electroanal. Chem.* **1996**, *404*, 237.
(3) Rolison, *D. R. Stud. Surf. Sci. Catal.* **1994**, *85*, 543.
(4) Dutta, P. K.; Ledney, M. *Prog. Inorg. Chem.* **1997**, *44*, 2209.
(5) Shaw, B. R.; Creasy, K. E.; Lanczycki, C. J.; Sargeant, J. A.; Tirhado, M. *J. Electrochem. Soc.* **1988**, *135*, 869.
(6) Gemborys, H. A.; Shaw, B. R. *J. Electroanal. Chem.* **1986**, *95*, 208.
(7) Li, Z.; Mallouk, T. E. *J. Phys. Chem.* **1987**, *91*, 643.
(8) Li, Z.; Wang, C. M.; Persaud, L.; Mallouk, T. E. *J. Phys. Chem.* **1988**, *92*, 2592.
(9) Baker, M. D.; Senaratne, C.; McBrien, M. *J. Phys. Chem.* **1995**, *99*, 12367.
(10) Li, J.-W.; Pfanner, K.; Calzaferri, G. *J. Phys. Chem.* **1995**, *99*, 12368.
(11) Bedioui, F.; Devynck, J.; Balkus, K. J., Jr. *J. Phys. Chem. B* **1996**, *100*, 8607.
(12) Senaratne, C.; Baker, M. D.; Zhang, J.; Bessel, C. A.; Rolison, D. R. *J. Phys. Chem. B* **1996**, *100*, 8610.
(13) Baker, M. D.; Senaratne, C.; Zhang. J. *J. Chem. Soc., Faraday Trans.* **1992**, *88*, 3187.
(14) Baker, M. D.; Senaratne, C.; Zhang. J. *J. Phys. Chem.* **1994**, *98*, 1668.
(15) Brouwer, D. H.; Baker, M. D. *J. Phys. Chem.* **1997**, *101*, 10390.
(16) Baker, M. D.; McBrian, M.; Burgess, I. *J. Phys. Chem. B* **1998**, *102*, 2905.
(17) Hui, T.-W.; Baker, M. D. *J. Phys. Chem. B* **2002**, *106*, 827.
(18) Bedioui, F.; De Boysson, E.; Devynck, J.; Balkus, K. J., Jr. *J. Chem. Soc., Faraday Trans.* **1991**, *87*, 3831.
(19) Bedioui, F.; De Boysson, E.; Devynck, J.; Balkus, K. J., Jr. *J. Electroanal. Chem.* **1991**, *315*, 313.
(20) Gaillon, L.; Sajot, N.; Bedioui, F.; Devynck, J.; Balkus, K. J., Jr. *J. Electroanal. Chem.* **1993**, *345*, 157.
(21) Bedioui, F.; Roué, L.; Briot, E.; Devynck, J.; Bell, S. L.; Balkus, K. J., Jr. *J. Electroanal. Chem.* **1994**, *373*, 19.
(22) Calzaferri, G.; Lanz, M.; Li, J.-W. *J. Chem. Soc., Chem. Commun.* **1995**, 1313.
(23) Li, J.-W.; Calzaferri, G. *J. Chem. Soc., Chem. Commun.* **1993**, 1430.
(24) Li, J.-W.; Calzaferri, G. *J. Electroanal. Chem.* **1994**, *377*, 163.
(25) Li, J.-W.; Pfanner, K.; Calzaferri, G. *J. Phys. Chem.* **1995**, *99*, 2119.
(26) Bessel, C. A.; Rolison, D. R. *J. Phys. Chem. B* **1997**, *101*, 1148.
(27) Bessel, C. A.; Rolison, D. R. *J. Am. Chem. Soc.* **1997**, *119*, 12673.
(28) Turro, N. J.; García-Garibay, M. In *Photochemistry in Organized Media*; Ramamurthy, V., Ed.; VCH: New York, 1991; pp 1−38.
(29) Doménech, A.; Formentín, P.; García, H. *J. Phys. Chem. B* **2002**, *106*, 574.
(30) Ramamurthy, V.; Caspar, J. V.; Corbin, D. R. *J. Am. Chem. Soc.* **1991**, *113*, 594.
(31) Corma, A.; García, H. *Top. Catal.* **1998**, *6*, 127.
(32) Corma, A.; Fornés, V.; García, H.; Miranda, M. A.; Primo, J.; Sabater, M. J. *J. Am. Chem. Soc.* **1994**, *116*, 2276.
(33) Sanjuán, A.; Alvaro, M.; Aguirre, G.; García, H.; Scaiano, H. *J. Am. Chem. Soc.* **1998**, *120*, 7351.
(34) Folgado, J.-V.; García, H.; Martí, V.; Esplá, M. *Tetrahedron* **1997**, *53*, 4947.
(35) Doménech, A.; Casades, I.; García, H. *J. Org. Chem.* **1999**, *64*, 3731.
(36) Doménech, A.; Doménech-Carbó, M. T.; García, H.; Galletero, M. S. *J. Chem. Soc., Chem. Commun.* **1999**, 2173.
(37) Doménech, A.; García, H.; Doménech-Carbó, M. T.; Galletero, M. S. *Anal. Chem.* **2002**, *74*, 569.
(38) Osteryoung, J.; O'Dea, J. J. In *Electroanalytical Chemistry*; Bard A. J., Ed.; Marcel Dekker: New York, 1986; Vol. 14, p 209.
(39) Lamaza, C.; Carbonell, E.; Narayana-Pillai, M.; Alvaro, M.; García, H. Submitted.
(40) Scholz, F.; Meyer, B. In *Electroanalytical Chemistry, A Series of Advances*; Bard, A. J., Rubinstein, I., Eds.; Marcel Dekker: New York, 1998; Vol. 20, pp 1−87.
(41) Zhang, J.; Lever, A. B. P.; Pietro, W. J. *Inorg. Chem.* **1994**, *33*, 1392.
(42) Soriaga, M. P. *Chem. Rev.* **1990**, *90*, 771.
(43) O'Dea, J. J.; Osteryoung, J.; Osteryoung, R. A. *Anal. Chem.* **1981**, *53*, 695.
(44) Lovric, M.; Komorsky-Lovric, M. S. *J. Electroanal. Chem.* **1988**, *248*, 239.
(45) Amatore, C.; Jutland, A.; Pflüger, F. *J. Electroanal. Chem.* **1987**, *218*, 361.
(46) Amatore, C.; Azzabi, M.; Calas, P.; Jutland, A.; Lefrou, C.; Rollin, Y. *J. Electroanal. Chem.* **1990**, *288*, 45.
(47) Zuman, P.; Perrin, C. L. *Organic Polarography*; Interscience: New York, 1969; pp 210−219.
(48) M'Halla, F.; Pinson, J.; Savéant, J.-M. *J. Am. Chem. Soc.* **1980**, *102*, 4120.
(49) Andrieux, C. P.; Hapiot, P.; Savéant, J.-M. *Chem. Rev.* **1990**, *90*, 723.
(50) Evans, J. F.; Blount, H. N. *J. Org. Chem.* **1977**, *42*, 976.
(51) Fleischmann, M.; Lasserre, F.; Robinson, J. *J. Electroanal. Chem.* **1984**, *177*, 115.
(52) Jones, G.; Huan, B.; Griffin, S. F. *J. Org. Chem.* **1993**, *58*, 2035.
(53) Kerr, G. T. *Zeolites* **1983**, *3*, 295.
(54) Amatore, C.; Jutland, A.; Pflüger, F.; Jallabert, C.; Strezelecka, H.; Weber, M. *Tetrahedron Lett.* **1989**, *30*, 1383.
(55) Couper, A. M.; Pletcher, D.; Walsh, F. C. *Chem. Rev.* **1990**, *90*, 837.
(56) Soriaga, M. P.; Hubbard, A. T. *J. Am. Chem. Soc.* **1982**, *104*, 2735.
(57) Daum, P.; Lenhard, J. R.; Rolison, D. R.; Murray, R. W. *J. Am. Chem. Soc.* **1980**, *102*, 4649.
(58) Bond, A. M.; Colton, R.; Daniels, F.; Fernando, D. R.; Marken, F.; Nagaosa, Y.; Van Stevenick, R. F. M.; Walter, J. N. *J. Am. Chem. Soc.* **1993**, *115*, 9556.